





Proceeding Paper

# Towards Low Temperature VOCs Chemoresistors: Graphene Oxide Versus Porphyrin-Based Materials †

Eleonora Pargoletti <sup>1,2</sup>, Francesca Tessore <sup>1,2</sup>, Gabriele Di Carlo <sup>1,2</sup>, Gian Luca Chiarello <sup>1</sup>  
and Giuseppe Cappelletti <sup>1,2,\*</sup>

<sup>1</sup> Dipartimento di Chimica, Università degli Studi di Milano, Via Golgi 19, 20133 Milano, Italy; eleonora.pargoletti@unimi.it (E.P.); francesca.tessore@unimi.it (F.T.); gabriele.dicarlo@unimi.it (G.D.C.); gianluca.chiarello@unimi.it (G.L.C.)

<sup>2</sup> Consorzio Interuniversitario Nazionale per la Scienza e Tecnologia dei Materiali (INSTM), Via Giusti 9, 50121 Florence, Italy

\* Correspondence: giuseppe.cappelletti@unimi.it; Tel.: +39-0250314228

† Presented at the 1st International Electronic Conference on Chemical Sensors and Analytical Chemistry, 1–15 July 2021; Available online: <https://csac2021.sciforum.net/>.

**Abstract:** The sensing of gas molecules is of fundamental importance for environmental monitoring, the control of chemical processes, and non-invasive medical diagnostics based on breath analysis in humans. Herein, the synthesis of hybrid materials (SnO<sub>2</sub>/graphene oxide-GO and SnO<sub>2</sub>/porphyrins composites) with ad hoc properties led to chemoresistors able to reduce the acetone sensing temperature, guaranteeing acceptable LOD values. As such, boosted potentialities, especially in terms of tuned selectivity and low water interference, may be obtained.

**Keywords:** VOC chemoresistors; hybrid materials; low-T sensing



**Citation:** Pargoletti, E.; Tessore, F.; Carlo, G.D.; Chiarello, G.L.; Cappelletti, G. Towards Low Temperature VOCs Chemoresistors: Graphene Oxide Versus Porphyrin-Based Materials. *Chem. Proc.* **2021**, *5*, 60. <https://doi.org/10.3390/CSAC2021-10418>

Academic Editor: Elisabetta Comini

Published: 30 June 2021

**Publisher's Note:** MDPI stays neutral with regard to jurisdictional claims in published maps and institutional affiliations.



**Copyright:** © 2021 by the authors. Licensee MDPI, Basel, Switzerland. This article is an open access article distributed under the terms and conditions of the Creative Commons Attribution (CC BY) license (<https://creativecommons.org/licenses/by/4.0/>).

## 1. Introduction

Volatile Organic Compounds (VOCs) are a huge class of molecules emitted from a large variety of both biogenic and anthropogenic sources [1]. They are considered as a critical factor for air pollution, and they give rise to serious problems for both the environment and human health [1,2] due to their easy diffusivity, volatility, and toxicity even at low concentrations [3]. Moreover, some VOCs, present in the human's breath can be considered as biomarkers of specific illnesses, as they are strictly correlated to several metabolic processes. Among them, acetone can be considered a biomarker for type I diabetes as its concentration in breath varies from 300 to 900 ppb in healthy people to more than 1800 ppb for diabetics [4].

For all these reasons, the monitoring of these compounds has become mandatory. A promising solution for the detection and quantification of VOCs consists in the implementation of chemoresistive gas sensors, based on the electrical resistance variation of the sensing material in the presence of target molecules. The key to facing this challenge is the development of miniaturized chemical sensors, capable of selective sensing a few ppb of VOCs, giving stable and reproducible responses in the presence of high concentrations of interfering species, such as water vapor and other gases [5].

Notably, n-type semiconductor metal oxide (MOS such as SnO<sub>2</sub>, WO<sub>3</sub>, ZnO, and TiO<sub>2</sub>) devices have already been used quite extensively for several applications. They are compact, low-cost, easy to produce and use, and able to detect a wide variety of gaseous species [6,7]. Although these features make such kind of sensors a convenient alternative to the traditional and most sophisticated analytical techniques (e.g., mass spectrometry and gas chromatography), there are also some drawbacks. Specifically, they can only operate at high temperatures (200–400 °C), showing short lifetime and low selectivity, so that it is difficult to selectively analyze multiple species in complex matrices [3].

To overcome these problems, the coupling of metal oxides with other matrices (such as carbonaceous- or porphyrin-based materials) [8,9] seems to be the key factor to create nano-composites capable of sensing at low temperatures ( $<100\text{ }^{\circ}\text{C}$ ), simultaneously achieving good selectivity and sensitivity (ppb level) towards a target compound.

Therefore, the present work is aimed at evaluating and comparing the sensing performances of  $\text{SnO}_2$  coupled with different porphyrins and graphene oxide (GO) towards acetone molecules, at mild temperatures ( $150\text{ }^{\circ}\text{C}$  and  $75\text{ }^{\circ}\text{C}$ ) under UV light, in a fixed  $\text{SnO}_2$ /matrix weight ratio.

## 2. Materials and Methods

### 2.1. Hybrid Synthesis, Electrodes Preparation and Sensing Tests

$\text{SnO}_2$  nanoparticles were chosen to be grown onto graphene oxide (GO) material by following a very easy hydrothermal method, already reported in our previous works [6–8]. According to earlier studies, we adopted 32:1 salt precursor-to-GO weight ratio since it resulted as the optimal one in terms of sensing performances at low operating temperatures [3].

Three different  $\text{Zn}^{\text{II}}$  porphyrins were synthesized according to previous papers [10–12], namely ZnTPP, ZnTPP( $\text{F}_{20}$ ), and ZnTPP( $\text{F}_{20}\text{CN}$ ); their relative chemical structures together with the UV-Vis spectra in  $\text{CH}_2\text{Cl}_2$  solution are reported in Figure 1. The UV-Vis patterns are the ones typically observed for porphyrins metal complexes [13], with an intense ( $\epsilon \approx 10^5\text{ M}^{-1}\text{ cm}^{-1}$ ) Soret or B band at 400–450 nm and two weaker ( $\epsilon \approx 10^3\text{--}10^4\text{ M}^{-1}\text{ cm}^{-1}$ ) Q bands at 500–600 nm (see the inset in Figure 1).

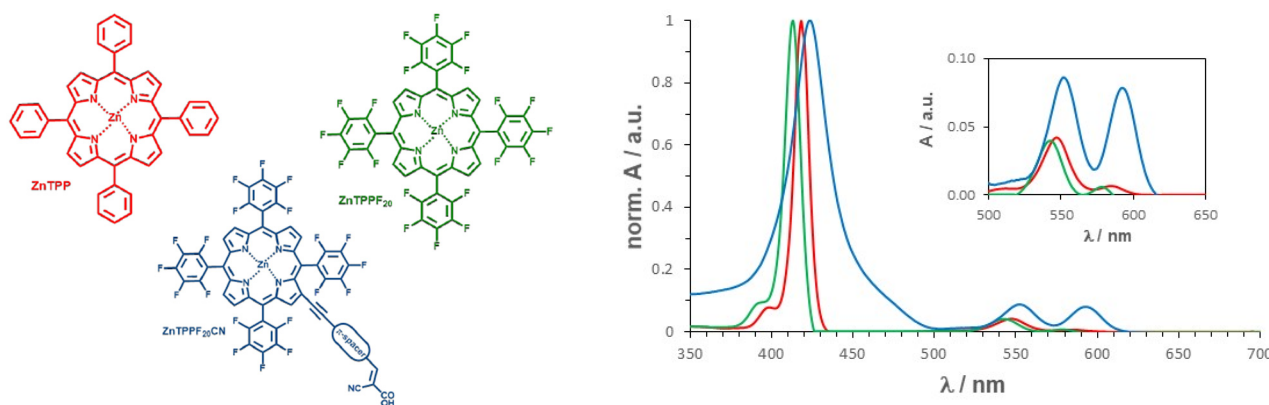


**Figure 1.** Investigated  $\text{Zn}^{\text{II}}$  porphyrins and their UV-Vis spectra.

Then, the  $\text{SnO}_2$ -porphyrin sensors were obtained by depositing onto Pt-based interdigitated electrodes (IDEs), through a hot-spraying method [6–8], a first layer of porphyrin ( $0.6\text{ mg mL}^{-1}$  in EtOH) followed by a thin film of  $\text{SnO}_2$  ( $2.5\text{ mg mL}^{-1}$  in EtOH). The mass ratio between  $\text{SnO}_2$  and porphyrin (verified by a microbalance) is 32:1 as in the case of the  $\text{SnO}_2$ /GO composite.

Sensing measurements towards acetone at  $150\text{ }^{\circ}\text{C}$  and  $75\text{ }^{\circ}\text{C}$  under UV light (Jelosil HG500 lamp; effective irradiation power:  $30\text{ mW cm}^{-2}$ ) were performed, adopting the chamber, already described elsewhere [14]. The tests have been carried up to  $150\text{ }^{\circ}\text{C}$  since the porphyrin complexes degrade at higher temperatures [15]. The sensor response is reported as:  $(R_{\text{air}}/R_{\text{acetone}}) - 1$ , where  $R_{\text{air}}$  is the film resistance in air and  $R_{\text{acetone}}$  is the film resistance at a given concentration of the acetone gas. We also computed the sensor response ( $t_{\text{res}}$ ) and the recovery times ( $t_{\text{rec}}$ ).

### 2.2. Powders and Porphyrins Characterizations

$\text{SnO}_2$  and  $\text{SnO}_2$ /GO samples were characterized by specific surface area measurements (Micromeritics Tristar II 3020, (Norcross, GA, USA), X-ray Powder Diffraction (XRPD, Philips PW 3710, Texas City, TX, USA) analyses and Diffuse Reflectance Spectroscopy (DRS,

Shimadzu UV-2600, Kyoto, Japan) to evaluate powders optical band gaps ( $E_g$ ) by means of Kubelka-Munk equation [3,8].

The goodness of the as-synthesized powders has been verified through  $^1\text{H}$ - and  $^{19}\text{F}$ -NMR spectroscopy in  $\text{CDCl}_3$ . The NMR spectra are fully in agreement with the recent literature [10–12].

### 3. Results and Discussion

Hybrid sensing materials, such as  $\text{SnO}_2$ -porphyrins and  $\text{SnO}_2$ -graphene oxide composites, arouse interest thanks to the possible complementary features between the two components, showing cooperative and synergistic behavior [6,9].

In the case of  $\text{SnO}_2/\text{GO}$  hybrid, the formation of nano-heterojunctions with a three-dimensional  $\text{SnO}_2$  network has been verified by a combination of physical and chemical characterizations. Specifically, Table 1 reports the specific surface area ( $S_{\text{BET}}$ ), together with total pores volume ( $V_{\text{tot. pores}}$ ), the average domain size by X-ray diffraction analysis ( $\langle d^{\text{XRPD}} \rangle$ ) and optical band gap ( $E_g$ ) of pure  $\text{SnO}_2$  and GO, together with the composite ( $\text{SnO}_2/\text{GO}$ ) sample. Moreover, HRTEM, XPS, Raman and responsivity analyses (already reported in our previous works [3,8]) corroborate that a nano-heterojunction occurs when tin oxide particles are grown onto GO sheets, allowing an intimate contact between the semiconductor and the graphene oxide matrix. This fact leads to a signal intensity of three times higher with respect to that of the pure  $\text{SnO}_2$  (Figure 2a) in the case of 20 ppm of acetone at 150 °C under UV light. Notably, the  $\text{SnO}_2/\text{GO}$  was able to reach a LOD of 100 ppb of acetone thanks to the synergistic effect between n-type MOS and p-type GO [3,6]. Furthermore, the response ( $t_{\text{res}}$  around 60 s) and recovery ( $t_{\text{rec}}$  around 90 s) times seem to be comparable with those of pure  $\text{SnO}_2$ .

**Table 1.** Surface area ( $S_{\text{BET}}$ ), total pore volume ( $V_{\text{tot. pores}}$ ), crystallite domain size by XRD analysis ( $\langle d^{\text{XRPD}} \rangle$ ) and optical band gap ( $E_g$ , by Kubelka-Munk extrapolation).

Sample	$S_{\text{BET}}$ ( $\text{m}^2 \text{g}^{-1}$ )	$V_{\text{tot. pores}}$ ( $\text{cm}^3 \text{g}^{-1}$ )	$\langle d^{\text{XRPD}} \rangle$ (nm)	$E_g$ (eV)
GO	30	0.020	11	—
$\text{SnO}_2$	67	0.210	15	3.6
$\text{SnO}_2/\text{GO}$	55	0.133	8	3.4

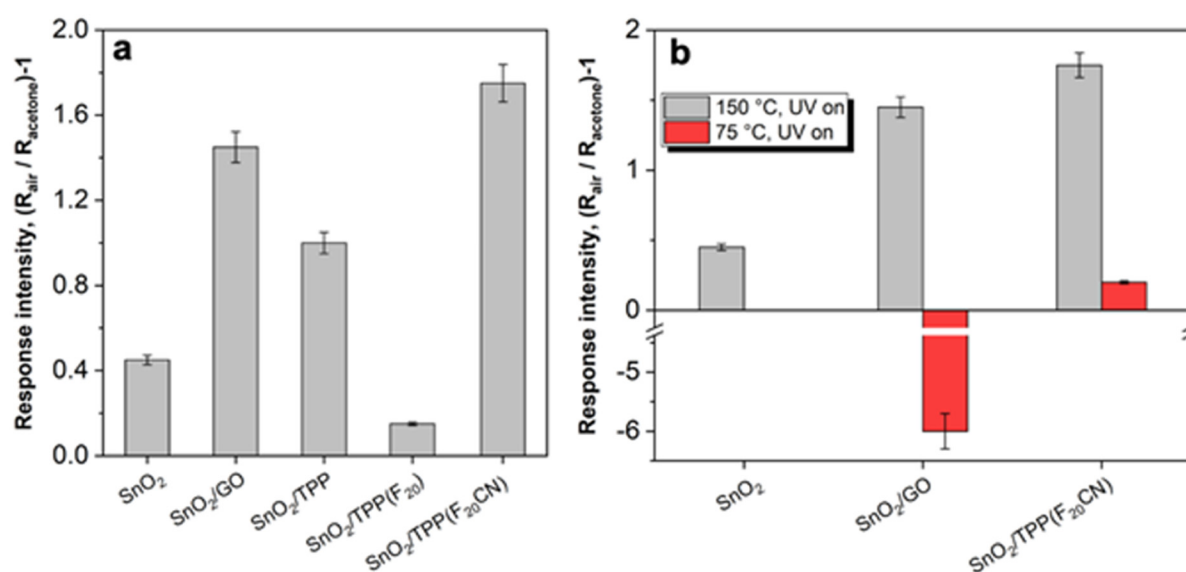


**Figure 2.** Sensor response intensities for both pure  $\text{SnO}_2$  and hybrid materials towards 20 ppm of acetone under UV light at (a) 150 °C and (b) 75 °C.

Then, the sensors obtained overlapping a SnO<sub>2</sub> and porphyrin layers were tested. Specifically, to evaluate the effect of the porphyrin matrix on the sensing properties of SnO<sub>2</sub>, the responses of SnO<sub>2</sub>/ZnTPP and SnO<sub>2</sub>/ZnTPP(F<sub>20</sub>) were compared to that of pristine SnO<sub>2</sub> as shown in Figure 2a. The combination of SnO<sub>2</sub> with the ZnTPP porphyrin matrix has undoubtedly a beneficial effect on the sensing performance, as reported in the recent literature [9,15,16]. Li et al. observed that light has a beneficial influence in the gas sensing by ZnO nanorods functionalized with porphyrins [16]. They asserted that light activates a charge transfer from the porphyrin to the ZnO, simultaneously creating a depletion of electrons, which favors the charge transfer from the donor-absorbed species.

Moreover, the main interfering species in the gas sensing process is humidity, especially at low T: Chen et al. [17] observed that the moisture can adsorb on the semiconductor oxide surface, interacting with the acetone molecules and leading to a dramatic change in the final sensor behavior. Indeed, a fluorine modified porphyrin, named as SnO<sub>2</sub>/ZnTPP(F<sub>20</sub>), was synthesized and tested, since fluorine atoms may confer hydrophobic character leading to a possible reduction of the water interference. Unfortunately, no positive results were obtained and the signal intensity halved compared to that of the pure SnO<sub>2</sub> powders, probably due to the strong electron density attractor capability of F-groups [10–12]. Notably, the sensor response of SnO<sub>2</sub>/ZnTPP(F<sub>20</sub>CN) at 150 °C (Figure 2a) is the most intense one among the tested hybrid materials, since this Zn<sup>II</sup> porphyrin carries a cyano-acrylic moiety able to bind SnO<sub>2</sub> and to impart a proper directionality to charge-injection [11,12]. Moreover, the CN group acts as a buffer towards the strong electron acceptor behavior of F atoms, guaranteeing concomitantly the desired hydrophobicity to prevent the water interference. All the porphyrin-based sensors reached LOD values of 200 ppb at 150 °C, notwithstanding an increase in the response times of around 25–30% and the recovery times significantly longer (around 200 s).

Finally, further tests were carried out at 75 °C (Figure 2b): while no acetone response (20 ppm) was appreciable in the case of pure SnO<sub>2</sub>, a reversed behavior in conductance with SnO<sub>2</sub>/GO sample occurred. This phenomenon is reported to be typical of metal oxide semiconductors, operating at low temperatures due to a greater amount of adsorbed oxygen species and moisture [17]. Instead, under these conditions SnO<sub>2</sub>/ZnTPP(F<sub>20</sub>CN) produces a positive response, even if the LOD is 600 ppb, corroborating the synergistic effect between the fluorine species and the anchor group.

We believe that these findings can provide guidelines for the engineering of miniaturized chemoresistive sensors for low-temperature detection of acetone molecule. The excellent performances of the SnO<sub>2</sub>-GO nano-heterojunctions and especially of SnO<sub>2</sub>/ZnTPP(F<sub>20</sub>CN) composite can pave the way for the development of tunable low-cost materials for the fabrication of optoelectronic devices for various applications.

**Author Contributions:** Conceptualization, E.P., F.T. and G.C.; methodology, E.P., G.L.C. and G.D.C.; validation, E.P.; formal analysis, E.P.; investigation, E.P.; data curation, E.P. and G.D.C.; writing—original draft preparation, G.D.C.; writing—review and editing, E.P., F.T. and G.D.C.; supervision, G.D.C. All authors have read and agreed to the published version of the manuscript.

**Funding:** This work received financial support from the Università degli Studi di Milano through the “PSR2019 Azione A” projects.

**Institutional Review Board Statement:** Not applicable.

**Informed Consent Statement:** Not applicable.

**Data Availability Statement:** Data are contained within the article.

**Conflicts of Interest:** The authors declare no conflict of interest.

## References

1. Guo, Y.; Wen, M.; Li, G.; An, T. Recent advances in VOC elimination by catalytic oxidation technology onto various nanoparticles catalysts: A critical review. *Appl. Catal. B Environ.* **2021**, *281*, 119447. [[CrossRef](#)]
2. Ren, F.; Gao, L.; Yuan, Y.; Zhang, Y.; Alqrni, A.; Al-Dossary, O.M.; Xu, J. Enhanced BTEX gas-sensing performance of CuO/SnO<sub>2</sub> composite. *Sens. Actuators B Chem.* **2016**, *223*, 914–920. [[CrossRef](#)]
3. Pargoletti, E.; Hossain, U.H.; Di Bernardo, I.; Chen, H.; Tran-Phu, T.; Chiarello, G.L.; Lipton-Duffin, J.; Pifferi, V.; Tricoli, A.; Cappelletti, G. Engineering of SnO<sub>2</sub>–Graphene Oxide Nanoheterojunctions for Selective Room-Temperature Chemical Sensing and Optoelectronic Devices. *ACS Appl. Mater. Interfaces* **2020**, *12*, 39549–39560. [[CrossRef](#)] [[PubMed](#)]
4. Güntner, A.T.; Abegg, S.; Königstein, K.; Gerber, P.A.; Schmidt-Trucksäss, A.; Pratsinis, S.E. Breath Sensors for Health Monitoring. *ACS Sens.* **2019**, *4*, 268–280. [[CrossRef](#)] [[PubMed](#)]
5. Tricoli, A.; Nasiri, N.; De, S. Wearable and Miniaturized Sensor Technologies for Personalized and Preventive Medicine. *Adv. Funct. Mater.* **2017**, *27*, 1605271. [[CrossRef](#)]
6. Pargoletti, E.; Hossain, U.H.; Di Bernardo, I.; Chen, H.; Tran-Phu, T.; Lipton-Duffin, J.; Cappelletti, G.; Tricoli, A. Room-temperature photodetectors and VOC sensors based on graphene oxide-ZnO nano-heterojunctions. *Nanoscale* **2019**, *11*, 22932–22945. [[CrossRef](#)] [[PubMed](#)]
7. Pargoletti, E.; Verga, S.; Chiarello, G.L.; Longhi, M.; Cerrato, G.; Giordana, A.; Cappelletti, G. Exploring Sn<sub>x</sub>Ti<sub>1-x</sub>O<sub>2</sub> Solid Solutions Grown onto Graphene Oxide (GO) as Selective Toluene Gas Sensors. *Nanomaterials* **2020**, *10*, 761. [[CrossRef](#)]
8. Pargoletti, E.; Tricoli, A.; Pifferi, V.; Orsini, S.; Longhi, M.; Guglielmi, V.; Cerrato, G.; Falciola, L.; Derudi, M.; Cappelletti, G. An electrochemical outlook upon the gaseous ethanol sensing by graphene oxide-SnO<sub>2</sub> hybrid materials. *Appl. Surf. Sci.* **2019**, *483*, 1081–1089. [[CrossRef](#)]
9. Ekrami, M.; Magna, G.; Emam-djomeh, Z.; Yarmand, M.S.; Paolesse, R.; Di Natale, C. Porphyrin-Functionalized Zinc Oxide Nanostructures for Sensor Applications. *Sensors* **2018**, *18*, 2279. [[CrossRef](#)] [[PubMed](#)]
10. Di Carlo, G.; Orbelli Biroli, A.; Pizzotti, M.; Tessore, F.; Trifiletti, V.; Ruffo, R.; Abboto, A.; Amat, A.; De Angelis, F.; Mussini, P.R. Tetraryl ZnII porphyrinates substituted at β-pyrrolic positions as sensitizers in dye-sensitized solar cells: A comparison with meso-substituted push-pull ZnII porphyrinates. *Chem. Eur. J.* **2013**, *19*, 10723–10740. [[CrossRef](#)] [[PubMed](#)]
11. Orbelli Biroli, A.; Tessore, F.; Di Carlo, G.; Pizzotti, M.; Benazzi, E.; Gentile, F.; Berardi, S.; Bignozzi, C.A.; Argazzi, R.; Natali, M.; et al. Fluorinated Zn<sup>II</sup> porphyrins for dye-sensitized aqueous photoelectrosynthetic cells. *ACS Appl. Mater. Interfaces* **2019**, *11*, 32895–32908. [[CrossRef](#)] [[PubMed](#)]
12. Berardi, S.; Caramori, S.; Benazzi, E.; Zabini, N.; Niorettini, A.; Orbelli Biroli, A.; Pizzotti, M.; Tessore, F.; Di Carlo, G. Electronic properties of electron-deficient Zn(II) porphyrins for HBr splitting. *Appl. Sci.* **2019**, *9*, 2739. [[CrossRef](#)]
13. Di Carlo, G.; Orbelli Biroli, A.; Tessore, F.; Pizzotti, M.; Mussini, P.R.; Amat, A.; De Angelis, F.; Abboto, A.; Trifiletti, V.; Ruffo, R. Physicochemical investigation of the panchromatic effect on β-substituted Zn<sup>II</sup> porphyrinates for DSSCs: The role of the π bridge between a dithienylethylene unit and the porphyrinic ring. *J. Phys. Chem. C* **2014**, *118*, 7307–7320. [[CrossRef](#)]
14. Americo, S.; Pargoletti, E.; Soave, R.; Cargnoni, F.; Trioni, M.I.; Chiarello, G.L.; Cerrato, G.; Cappelletti, G. Unveiling the acetone sensing mechanism by WO<sub>3</sub> chemiresistors through a joint theory-experiment approach. *Electrochim. Acta* **2021**, *371*, 137611. [[CrossRef](#)]
15. Anjali, K.; Jayaraj, L.K.N.; Ayyamperumal, C. Zinc-tetraphenylporphyrin grafted on functionalised mesoporous SBA-15: Synthesis and utilisation for nitroaldol condensation. *J. Porous Mater.* **2020**, *27*, 1191–1201. [[CrossRef](#)]
16. Li, X.; Cheng, Y.; Kang, S.; Mu, J. Preparation and enhanced visible light-driven catalytic activity of ZnO microrods sensitized by porphyrin heteroaggregate. *Appl. Surf. Sci.* **2010**, *256*, 6705–6709. [[CrossRef](#)]
17. Chen, H.; Bo, R.; Shrestha, A.; Xin, B.; Nasiri, N.; Zhou, J.; Di Bernardo, I.; Dodd, A.; Saunders, M.; Lipton-Duffin, J.; et al. NiO–ZnO Nanoheterojunction Networks for Room-Temperature Volatile Organic Compounds Sensing. *Adv. Opt. Mater.* **2018**, *6*, 1800677. [[CrossRef](#)]